

TWO AXIS CLOSED-LOOP ANTENNA POINTING FOR A DUAL-SPIN SPACECRAFT

John W. Smay
Manager, Systems Design Department
Space and Communications Group
Hughes Aircraft Company
El Segundo, California

ABSTRACT

This paper describes the control and sensing techniques and practical implementation used to obtain precision antenna pointing on a class of commercial communication satellites. The basic spacecraft bus is a dual-spin gyrostator with momentum of order 1500 ft-lb-sec. Spin is about a minimum axis of inertia and active damping using the despin motor and platform product of inertia is employed for nutation stabilization. Using two axis RF beacon tracking, steady state pointing accuracy exceeding 0.025° (3σ) in roll and pitch and 0.1° (3σ) in yaw is achieved. This accuracy is approached during orbit and attitude trim thrusting maneuvers as well.

INTRODUCTION

A new family of dual-spin spacecraft provides a greater than 75% reduction of pointing error over comparable predecessor commercial satellites. This vehicle is being flown for Satellite Business Systems (SBS), ANIK C, and five other commercial communications missions. The first spacecraft was launched for SBS on November 15, 1980 with a 10 transponder K-band (12/14 GHz) payload. Sixteen additional spacecraft are being built for six customers with K and C band payloads. The spacecraft bus is generally compatible with Space Shuttle, Delta 3910, and Ariane launch vehicles.

This paper addresses primarily attitude and pointing control aspects of the spacecraft. A sketch of the vehicle highlighting attitude control elements is shown by Figure 1. Pointing accuracy of ± 0.025 deg (3σ) in roll and pitch, is achieved by closed-loop beacon tracking in two axes. Roll and pitch sensing is provided by tracking a ground beacon with the communications antenna reflector and four feedhorns. Pitch motion of the boresight is obtained via the despin bearing and roll motion by gimbaling the antenna reflector. These gimbaling elements are shown in Figure 1. Yaw pointing accuracy of 0.1 deg (3σ) is obtained by gyroscopic stiffness provided by 1000-1400 ft-lb-sec of momentum in the

spinning rotor combined with open loop ground commanded attitude (momentum) trim maneuvers.

A rather detailed mission sequence description has been given in (1). Here we include only the following brief sketch. At launch and throughout the transfer orbit used to attain synchronous orbit the spacecraft is an allspun single body with the antenna reflector and telescoping solar drum extension stowed. Subsequent to perigee motor ejection in this configuration the vehicle has spin to transverse inertia ratio greater than unity and therefore exhibits passive nutational stability (2). After apogee motor injection into near synchronous orbit the payload platform is unlocked and despun. By despinning the platform the inertia ratio is reduced to less than unity and active nutation stabilization is required for the remainder of the mission. Subsequent to platform despin the reflector and solar drum are deployed to the on station configuration depicted on Figure 1. Active nutation damping is provided by the despin active nutation damping electronics (DANDE). This control senses nutation with a rotor mounted accelerometer and commands despin motor torques, which couple through the despun product of inertia to produce transverse plane nutation damping torques. Theory of the DANDE is given in (3) and performance applicable to this spacecraft is reported in (1). A thruster actuated nutation control is also provided for large angle capture and backup purposes.

Initial despin of the platform and acquisition of the ground beacon is implemented by a rotor to platform relative rate control and an earth sensor referenced pitch position control. The earth sensor control provides backup pointing at lower accuracy in the event of ground beacon failure. The paper describes each of the pointing control loops and representative pointing error bounds. Also treated are control techniques and pointing errors associated with thrusting maneuvers for orbit and attitude trim.

ANTENNA POINTING CONTROL

A block diagram showing the functional interconnection of attitude control elements is shown as Figure 2. The despin motor for control of platform spin rate and East-West position is contained within the despin bearing assembly. Three East-West control modes are provided, viz, Rate, Earth Tracking, and Beacon Tracking. When locked on the ground beacon, the feedhorn arrangement and track receiver signal processing provides precision two axis pointing error sensing about East-West (pitch) and North-South (roll). Autonomous North-South pointing is implemented by stepping the antenna reflector with respect to the deployment mechanism. Each of the control loops is discussed individually below.

Rate Control

The rate control mode is used to initially despin the platform and maintain it closely despun during antenna and solar drum deployments. It also aids in E-W earth pointing acquisition, provides a safe and stable autonomous backup mode in the event of pointing loop failure, and serves as a stable control mode requiring no external sensor inputs for long term inactive on orbit storage of the satellite.

The despin bearing assembly contains redundant shaft angle encoders, each of which produce two equally spaced index pulses separated 180° in relative phase. The period of this pulse train is detected for use as a relative rate measurement. The rate measurement is compared with a ground commendable bias to derive despin motor torque commands which null platform to rotor relative rate at the selected value between 25 and 90 rpm. At the nominal 65 rpm rotor rate the bias is quantized at 0.3 rpm with the platform near the inertially despun condition.

Earth Pointing Control

The primary function of the earth sensor referenced despin control is to position the antenna with sufficient accuracy for acquisition of the ground beacon. This mode also serves as a temporary backup pointing control in the event of loss of ground beacon or failure of the spacecraft beacon tracker. Short term pointing accuracy is 0.16 deg. after on orbit calibration from the beacon, while uncalibrated accuracy is about 0.3 deg.

The earth position sensor is mechanized to detect offset of a relative phase index pulse from the midpoint of earth leading and trailing edge pulses generated by a rotor-mounted spinning earth sensor. The error is sampled at spin rate, and the loop produces stable control over a rotor spin range of 50 to 90 rpm. The sensor and index pulse are nominally positioned to point the antenna at earth center. The basic mechanization has been previously employed on a number of spacecraft and is detailed for Intelsat IV in (4). A ground selectable offset bias is provided with range approximately equal to the earth chord (± 7 deg) and 0.015 deg. quantization.

The attitude control electronics can be commanded to the Earth Mode from the ground or autonomously by onboard detection of failure in the beacon tracking loop. In Earth Mode the despin command torque can be obtained only from the position sensor, or as the sum of position and rate error torques. The former is true when the index pulse (\sim antenna boresight) is in the earth chord. When the index pulse is out of the earth chord the torque commands are summed with weighting such that the rate command has ultimate authority. This scheme provides automatic earth pointing acquisition from any relative rate at which the vehicle is nutationally stable, as well as automatic rate control takeover to maintain the platform closely despun should an earth sensor fail.

Beacon Pointing Control

Normal mode precision pointing of the antenna is accomplished by tracking an RF beacon transmitted from the ground control station. A brief description of the RF pointing error sensor is given below. This sensor produces two orthogonal E-W and N-S pointing error signals used as reference to the respective pointing loops. The beacon is initially acquired or reacquired during the mission by offset stepping pointing position in Earth Mode about two axes while monitoring telemetered RF lock and tracker pointing error signals on the ground. Once the antenna is appropriately positioned closed-loop control is transferred to the beacon separately about each axis by ground commands. Automatic detection and switching to the alternate unit is implemented in the event of ground beacon loss to the track receiver in control.

Total pointing error about each axis of less than $\pm 0.025^\circ$ is achieved in steady state when no thrusting maneuver transients are present. Since the same reflector-feedhorn structure is employed for beacon tracking and the communication function, biases and misalignments are largely eliminated from pointing error.

The beacon E-W error signal is transferred to the attitude control electronics on the spinning rotor via slip rings where it is processed by analog compensation to provide the despun control torque command. This forms a linear continuous loop with a 0.5 Hz bandwidth. The N-S beacon error signal is low-pass filtered to attenuate nutation, spin frequency, and noise components. It is then applied through a ± 0.0035 deg. deadband to drive an antenna positioning stepper motor. Mechanical steps are 0.0025 deg. and produce beacon boresight steps of about 0.005 deg. The N-S loop primarily tracks out spin axis attitude error and orbit inclination effects, with stepping rate of order one step per 10-20 minutes. The loop bandwidth is intentionally set low enough to decouple nutation and spin frequency from the stepper motor.

BEACON SENSOR DESCRIPTION

Power from a ground station RF beacon signal is received by a square array of four feedhorns and processed to produce two axis pointing error signals. A schematic diagram of the sensor is shown by Figure 3. Four magic tee power summers combine signals from the four feedhorns to produce sum, East-West difference (pitch), and North-South difference (roll) signals. The sum signal at point 2 of Figure 3 is passed through a directional linear phase filter which routes beacon frequencies to the downstream error signal processing and communication signal frequencies to the communications receiver. A combination of beacon uplink signal periodic frequency modulation at the transmitter, and a linear phase filter in the sum path allow the sum and difference signals to be recombined such that the result has orthogonal amplitude modulation components proportional to the two difference power (pointing error) signals. Details of the amplitude modulation scheme

are beyond the scope of this paper. Each of the two redundant Command/Track Receivers demodulates these orthogonal signals and provides base band two axis pointing error to the respective control systems. Typical error sensor characteristics are shown by Figure 4.

The four beacon feedhorns are part of a larger array which, along with the reflector, form the communications antenna pattern. As a part of the payload communications pattern the beacon receiver eliminates biases and long term deformations between sensor and pointed payload that might have to be accommodated with another sensor. In addition the beacon tracker is a very high bandwidth low noise sensor which permits design of a high bandwidth control loop for plant disturbance rejection.

Spacecraft command tones are also encoded on the beacon signal by frequency modulation and detected by the Command/Track Receivers. Commands are received through an omni antenna, shown in Figure 3 when the directional antenna is not locked on the beacon. The omni and beacon track paths are isolated by orthogonal polarization and/or frequency separation.

ON ORBIT THRUSTING MANEUVERS

All thrusting maneuvers are performed with four 5 lb monopropellant thrusters. Two radial thrusters are aligned to thrust through the average on station cm location with alternate thrusters having small (~ 10 deg.) spin up and spin down biases. Two axial thrusters have 1 deg. opposing spin biases and are aligned to produce about 2.6 ft transverse moment arms. Thruster locations are depicted on Figure 1. This section will primarily address antenna pointing performance induced by thrusting maneuvers. Some unique features of these maneuvers arise from the closed-loop N-S tracking and a substantial despun platform static imbalance.

Orbit velocity aspects of the stationkeeping maneuvers are standard for a dual spin vehicle. East-West velocity maneuvers are performed by pulsing a radial thruster as it spins past the orbit velocity vector. North-South velocity maneuvers are performed by simultaneously firing both axial thrusters for an appropriate period at the descending node. The spin torques produced by thruster cant cause small spin rate changes (< 0.1 rpm) during attitude trim and East-West velocity maneuvers. These spin changes are trimmed by selection of alternate thrusters on successive maneuvers or by special spin trim maneuvers. The thruster spin cants provide spin torque capability to adjust angular momentum during the mission sequence and, if required, for failure mode recovery, e.g., for flat spin recovery.

Attitude Trim

Spin axis (momentum vector) attitude trim maneuvers are performed periodically to unload accumulated momentum due to solar precession torque. This maneuver is accomplished by spin synchronous pulsing of one axial thruster in a manner analogous to many preceding dual-spin satellites (5). Trim maneuvers are performed at local noon or midnight such that the attitude error is entirely yaw, hence the N-S tracking servo does not have to follow the relatively rapid attitude correction. Pointing errors during the maneuver are limited to nutation induced by trim torque pulses plus some amplification in roll due to the dominant cantilever flexible mode of the antenna reflector. Mixed Simulation Test (MST) results of a simulated attitude trim maneuver are shown as Figure 5. The MST employs flight attitude control electronics connected in a closed-loop simulation with spacecraft sensors, actuators, and vehicle dynamics modeled using an analog computer and additional special purpose test equipment. Full non-linear equations with five degree-of-freedom rotational dynamics are modeled. The simulation runs in real time and represents on orbit performance with a high degree of fidelity. The maneuver consists of a train of 40 ms torque pulses. The first flexible mode of the antenna support structure and positioning mechanism is represented as a composite lumped parameter mode with frequency and damping ω_m , ζ_m as noted. Excitation of this mode is evident on Traces 5 and 7 of the simulation.

East West Stationkeeping

MST simulation variables for an East-West velocity maneuver are shown as Figure 6. The maneuver is executed by ground commanded firing of 117 ms radial thruster pulses centered over the orbit velocity vector. The thruster nominally passes through the vehicle cm. However, due to propellant consumption over the mission life, the cm moves axially creating a small moment arm with the thruster. This results in a small yaw torque, and corresponding roll precession, during the maneuver. The precession is evident in the platform roll motion shown on Figure 6, Trace 4. This motion is tracked out of boresight pointing error by the North-South tracking loop with a small offset due to servo time delay. Trace 5 shows the resultant pointing error, while Trace 7 shows the stepper motor control of platform to antenna relative position. The filtered stepper motor drive error signal is shown by Trace 6. Considerable excitation of the flexible mode described above is evident on Traces 5 and 7. The thruster pulsing rate on Figure 6 is one pulse every fifth spin period. The rate is chosen to simultaneously bound the precession rate (hence North-South tracking servo lag), and to be suitably asynchronous with nutation frequency to avoid excitation of excessive nutation. The pulsing rate is varied slightly over mission life to compensate for thrust and vehicle inertia ratio variations.

Attention is now turned to East-West pointing error induced by pulsing a radial thruster to execute the East-West velocity maneuver. As a result of the platform static imbalance

produced by the deployed antenna, the vehicle mass distribution in steady state (no thrusting) is as depicted on Figure 7 when viewed from the north end of the spin axis. The orbit velocity is denoted by \vec{v} and the thruster force by \vec{F} . For simplicity assume that \vec{F} passes through the vehicle cm such that it applies no external torque. It can be shown that when the thruster fires, an internal torque equal to the spin axis component of $\vec{r}_1 \times \vec{F}$ is applied along the bearing axis between the rotor and platform. Thus, the thrust pulses perturb East-West pointing in a manner identical to that which would be seen if such a pulse stream were applied as a command to the despun motor. Pointing response is determined by the torque disturbance response of the despun control loop. The simulated disturbance is shown by Trace 8 of Figure 6.

Reading from Traces 5 and 8 respectively of Figure 6, worst case North-South and East-West pointing errors induced by the maneuver are about ± 0.0125 deg. Yaw error is limited to the nutation induced by pulsing and the reaction to antenna North-South stepping. This is bounded to ± 0.003 deg., as may be verified by integrating Trace 3 of Figure 6.

North-South Stationkeeping

North-South stationkeeping maneuvers are nominally executed by continuous firing of both axial thrusters. Ignoring spin cant temporarily, the thrusters are symmetrically aligned in a plane containing the spin axis. Observe from Figure 7 that continuous firing of both thrusters produces a transverse platform fixed (inertial) torque along the roll axis (1-axis). The torque is equal to the transverse component of $2\vec{r}_1 \times \vec{F}$, where \vec{F} is the axial force from one thruster. If allowed to persist this torque would precess the momentum vector as much as 1. - 1.5 deg. in yaw over a 60 second velocity maneuver. To avoid this, each thruster is off-pulsed once per spin period as it passes the spacecraft to earth line. The pulsewidth is adjusted to produce zero average yaw torque and results in negligible yaw precession buildup.

In addition to the static imbalance inertial torque, two rotor fixed or spinning disturbance torques perturb pointing during North-South velocity maneuvers. The opposing spin cant of the two axial thrusters produces a transverse torque in the plane of the thrusters, and thrust mismatch of the two thrusters generates a torque normal to the latter. Figure 8 shows a digital simulation of small angle motion of the vehicle spin axis during a typical velocity maneuver. The coordinate bases on this figure indicate the relative positions and magnitudes of disturbance torques at the instant thrusting begins. In the figure e_p is a platform fixed basis and e_s is the spinning rotor fixed basis. The sign of the mismatch torque, which is unknown, is chosen arbitrarily,

Shown on Figure 9 are MST results obtained from simulation of the maneuver with flight electronics. Traces 1 and 2 indicate respectively relative phase of the rotor and platform

and the thrust profile with off-pulses. The next two traces show transverse rates in a despun platform (inertial) basis. Traces 6 and 7 show North-South pointing error and platform to antenna relative position respectively with the previously described 2.5 Hz flexible mode included. In the absence of flexibility, pointing error would be as indicated by Figure 8 (~ 0.01 deg.). The flexible mode effect produces errors approximately twice as large (~ 0.025 deg.). The last trace of Figure 9a shows the filtered North-South pointing error signal which drives the antenna positioning stepper rotor through the control deadband. Initial and terminal transients induced by thrusting produce a small amount of tracking steps, evident on Trace 7.

East-West pointing error effects of the maneuver are indicated on Figure 9b. The first and second traces show the raw and filtered acceleration from the rotor mounted axial nutation accelerometer. The long exponential component saturates the DANDE nutation damping path and is then chopped at spin rate (for DANDE frequency translation purposes explained in (3)) to produce the torque command of Trace 3. Subsequent to this simulation the 25 second acceleration filter time constant of Trace 2 has been changed to 2.5 seconds. Finally the resultant spin periodic effect of platform East-West pointing error is shown on Trace 4. For most missions the DANDE can be disabled for the short time span of this maneuver and spacecraft mutational stability provided by simple despun control coupling through the despun product of inertia (3). This eliminates the maneuver thrust acceleration coupling path completely, and reduces the East-West pointing transient by a factor of five or greater.

POINTING ACCURACY SUMMARY

North-South and East-West

In this section we discuss a representative summary pointing error budget for the two controlled axes. The budget is given by Table 1, where errors are grouped into categories determined by their frequency of variation. The constant or bias error is determined by the accuracy of ground calibration and quantization of the command employed to remove the bias on orbit. A small long term error buildup is allocated by analysis for component aging, radiation, and long term thermal effects in the sensor and control electronics.

Diurnal variations in the RF beacon sensor error are produced by thermal gradients due to the varying sun angle on the despun platform and reflector. Additionally, in eclipse season, more pronounced daily temperature cycles are induced on the entire spacecraft. Temperature cycling of the despun bearing can produce running friction changes and accompanying pointing variations.

Short term RF sensor reference error may be produced by atmospheric phenomena and beacon transmitter variations. Sensor noise from both the RF sensor and the nutation

sensing accelerometer produce small contributions to pointing error in the continuous drive E-W loop, while the N-S deadband makes a larger contribution to that axis. Disturbance torques are induced by despin bearing imperfections, antenna reflector N-S stepping, and rotor static imbalance. Finally, rotor dynamic imbalance induces spin axis coning or wobble which is maintained below 0.0025 deg. by on orbit dynamic balancing with the deployed solar drum as described in (1). Maneuver errors, which have been discussed at length above, are also tabulated on Table 1.

Yaw Pointing

On a spin stabilized spacecraft yaw pointing errors are of basically three types 1) initial alignment error, 2) diurnal cyclic errors due to orbit inclination and inertial misalignment (attitude) of the spin axis, and 3) spin and nutation frequency terms due to mass imbalance and thrust maneuver induced nutation. Spin axis attitude determination is performed by ground station processing of telemetered data from spinning earth and sun sensors. The technique is virtually identical to that used on many predecessor satellites and is described in (6). The desired attitude is maintained within a deadband by periodic ground commanded axial thruster pulses which dump accumulated momentum due to solar pressure.

In the absence of active roll pointing the spin axis attitude is typically maintained at orbit normal. An orbit inclination angle β then produces diurnal cyclic roll and yaw errors with peak excursion of $\beta / \{r_o/r_e - 1\} = 0.178\beta$ and β respectively (r_o and r_e are orbit and earth radius). This gives a roll error about 18% of the yaw error. If instead the spin axis is maintained equatorial normal the respective roll and yaw errors become $(\beta r_o/r_e / \{r_o/r_e - 1\}) = 1.178\beta$ and 0. Thus, with active roll tracking the spin axis is maintained equatorial normal and the cyclic roll error due to inclination is tracked out while the yaw contribution vanishes.

Spin and nutation frequency components for the subject satellite are about ± 0.02 deg. maximum. Combined measurement and control granularity is of order ± 0.035 deg. Yaw pointing error is maintained below the sum of these plus the secular attitude drift permitted between attitude trim maneuvers. Yaw accuracy better than ± 0.1 deg is planned for some applications.

CONCLUSION

A description is presented for a dual-spin spacecraft of the Gyrostat configuration which employs two axis closed loop active antenna pointing control. The primary sensor is a two axis RF beacon tracking system. This sensor gives excellent signal to noise characteristic for high bandwidth control, and since it is integral to the communications payload alignment and alignment stability errors are greatly reduced. A substantial improvement in

pointing accuracy, and hence communication performance, over prior commercial communication satellites is achieved with the control scheme described.

ACKNOWLEDGEMENT

The author acknowledges supporting consultation on the RF beacon sensor and beacon tracking aspects provided by Doug Burr and Bob Blink of Hughes Aircraft.

REFERENCES

- 1) Smay, J. W., "Attitude and Pointing Control of the SBS Communications Satellite Bus," presented at AAS Rocky Mountain Guidance and Control Conference, January 31, 1981, Paper No. AAS 81-043.
- 2) Likins, P. W., "Attitude Stability Criteria for a Dual-Spin Spacecraft," *Journal of Spacecraft and Rockets*, Vol. 4, April 1967, pp. 1638-1643.
- 3) Smay, J. W. and Slafer, L. I., "Dual-Spin Spacecraft Stabilization Using Nutation Feedback and Inertia Coupling," *Journal of Spacecraft and Rockets*, Vol. 13, No. 11, Nov. 1976, pp. 630-639.
- 4) Adams, G. J., "Communication Satellite Control Systems," Society of Automotive Engineers National Aerospace Engineering and Manufacturing Meeting, San Diego, Calif., October 1-3, 1974, SAE Paper No. 740-872.
- 5) Sierer, W. H., and Snyder, W. A., "Attitude Determination and Control of Syncom, Early Bird, and Applications Technology Satellites," *Journal of Spacecraft and Rockets*, Vol. 6 No. 2, February 1969, pp. 162-166.
- 6) Sierer, W. H. and Del Riego, J., "TACSAT Attitude Determination," Proceedings of the Symposium on Spacecraft Attitude Determination, Aerospace Report No. TR-0066 (5306)-12, Vol. 1, Los Angeles, Calif. September 30, 1969. pp. 235-247.

**TABLE 1. REPRESENTATIVE RF BEACON REFERENCE POINTING
ERROR BUDGET**

ERROR TYPE	ERROR BOUND DEGREES	
	E-W (PITCH)	N-S (ROLL)
CONSTANT		
RF SENSOR CALIBRATION	0.0047	0.0035
CONTROL SERVO OFFSET	0.001	0.001
COMMAND QUANTIZATION	0.001	0.001
RSS TOTAL	0.0049	0.0038
LONG TERM VARIATIONS		
THERMAL, RADIATION, AND AGING	0.0017	0.002
DIURNAL VARIATIONS		
RF SENSOR DRIFTS	0.004	.003
REFLECTOR THERMAL DISTORTION	.012	.012
BEARING FRICTION	0.001	--
RSS TOTAL	0.013	0.012
SHORT TERM VARIATIONS		
BEACON TRANSMITTER VARIATIONS	0.0012	0.001
SENSOR NOISE	0.0005	--
SERVO DEADBAND	–	0.0035
DISTURBANCE TORQUES	0.005	0.0002
WOBBLE	–	0.0025
RSS TOTAL	0.0052	0.0044
TOTAL ERROR IN STEADY STATE	0.025	0.023
MANEUVER TRANSIENT ERRORS		
E-W VELOCITY MANEUVER	0.01	0.007
N-S VELOCITY MANEUVER	0.02	0.028
ATTITUDE TRIM	0.007	0.025

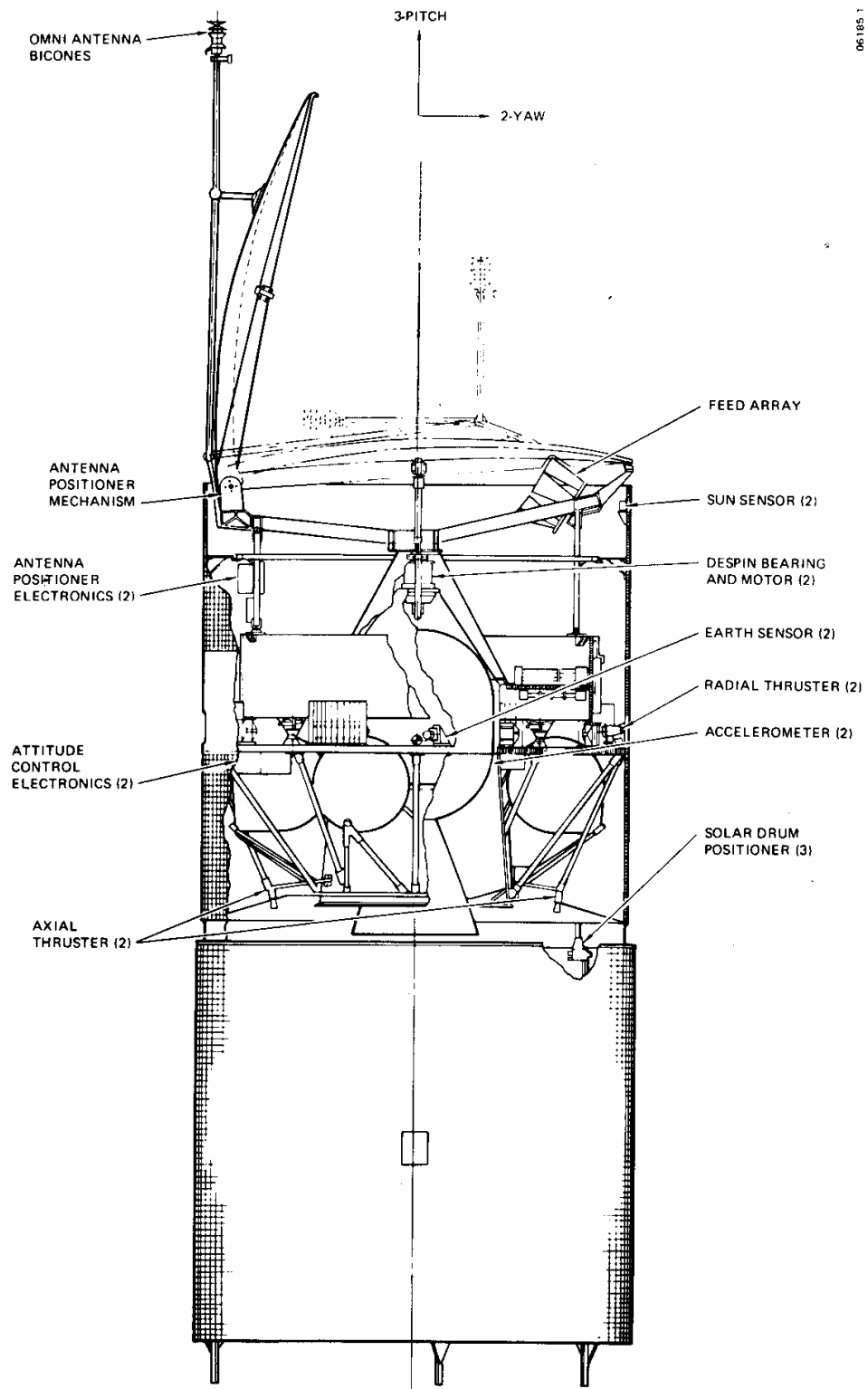


Figure 1. Spacecraft Configuration and Control Element Location

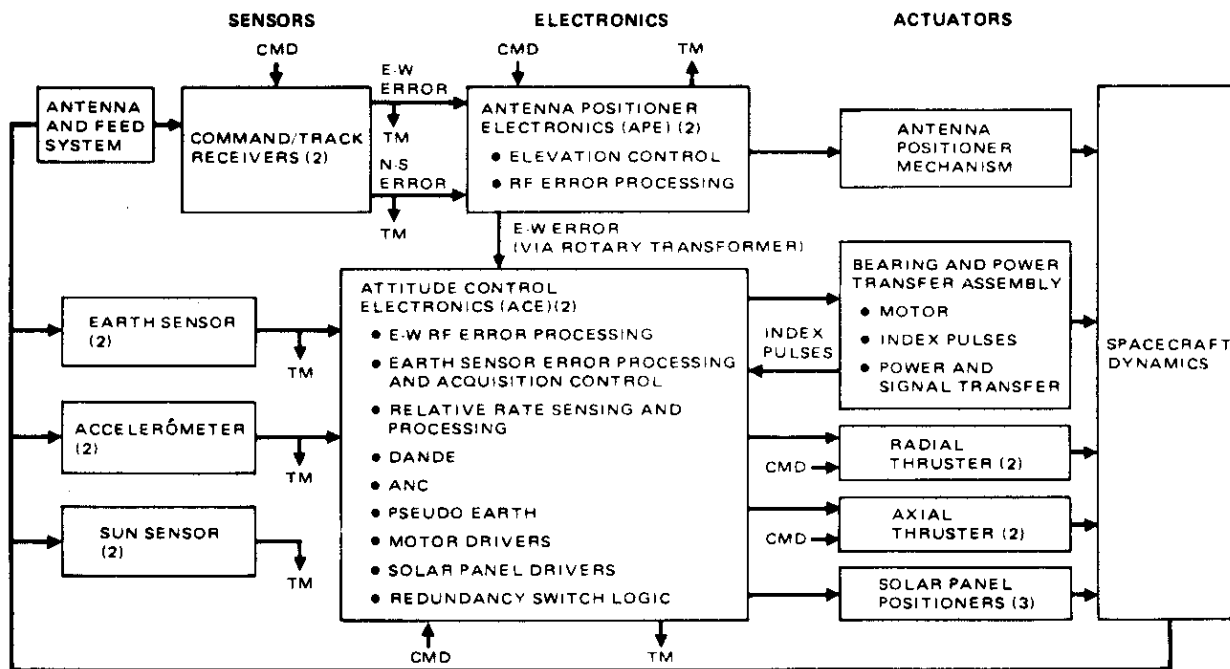


Figure 2. Attitude Control System Functional Block Diagram

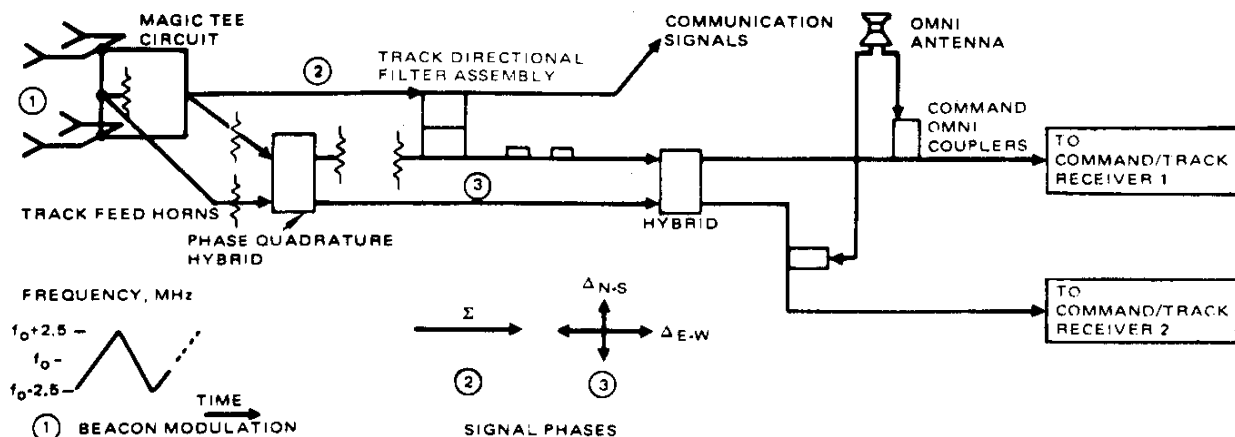


Figure 3. RF Beacon Track Network Schematic

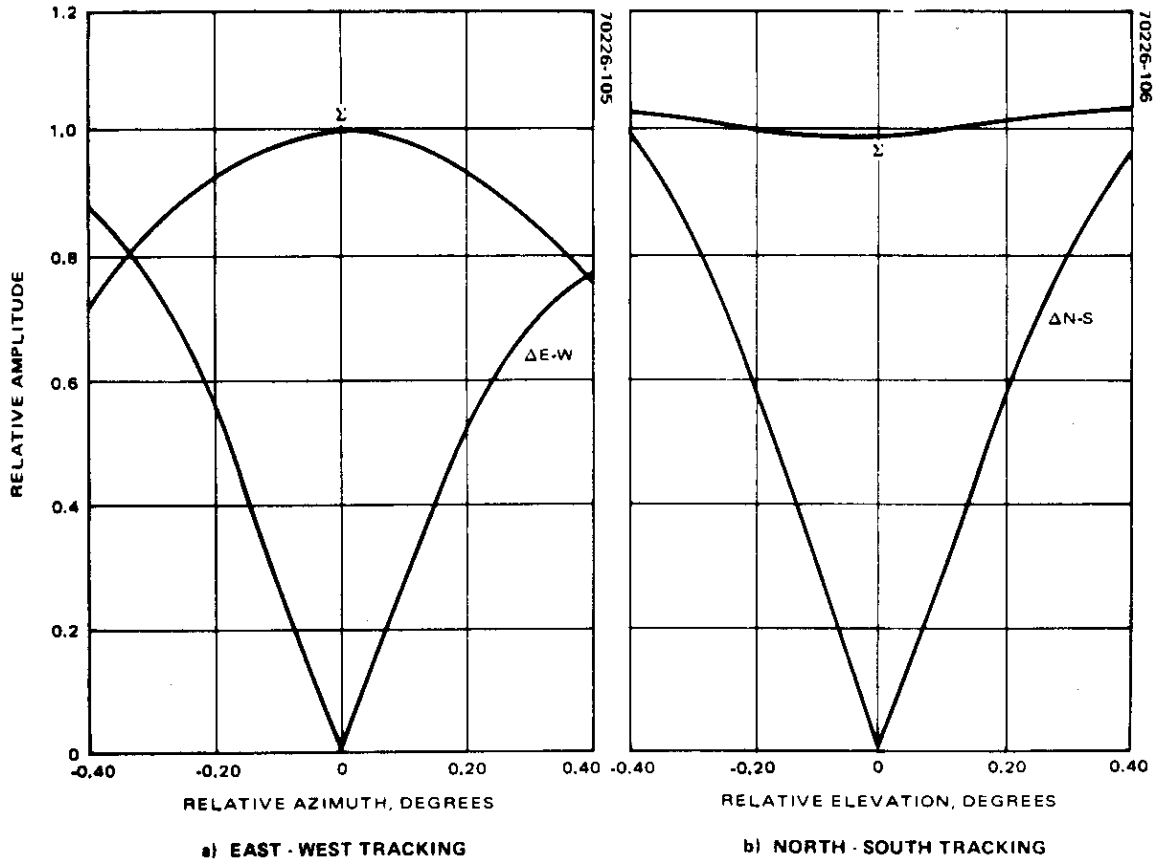


Figure 4. Beacon Error Sensor Characteristic

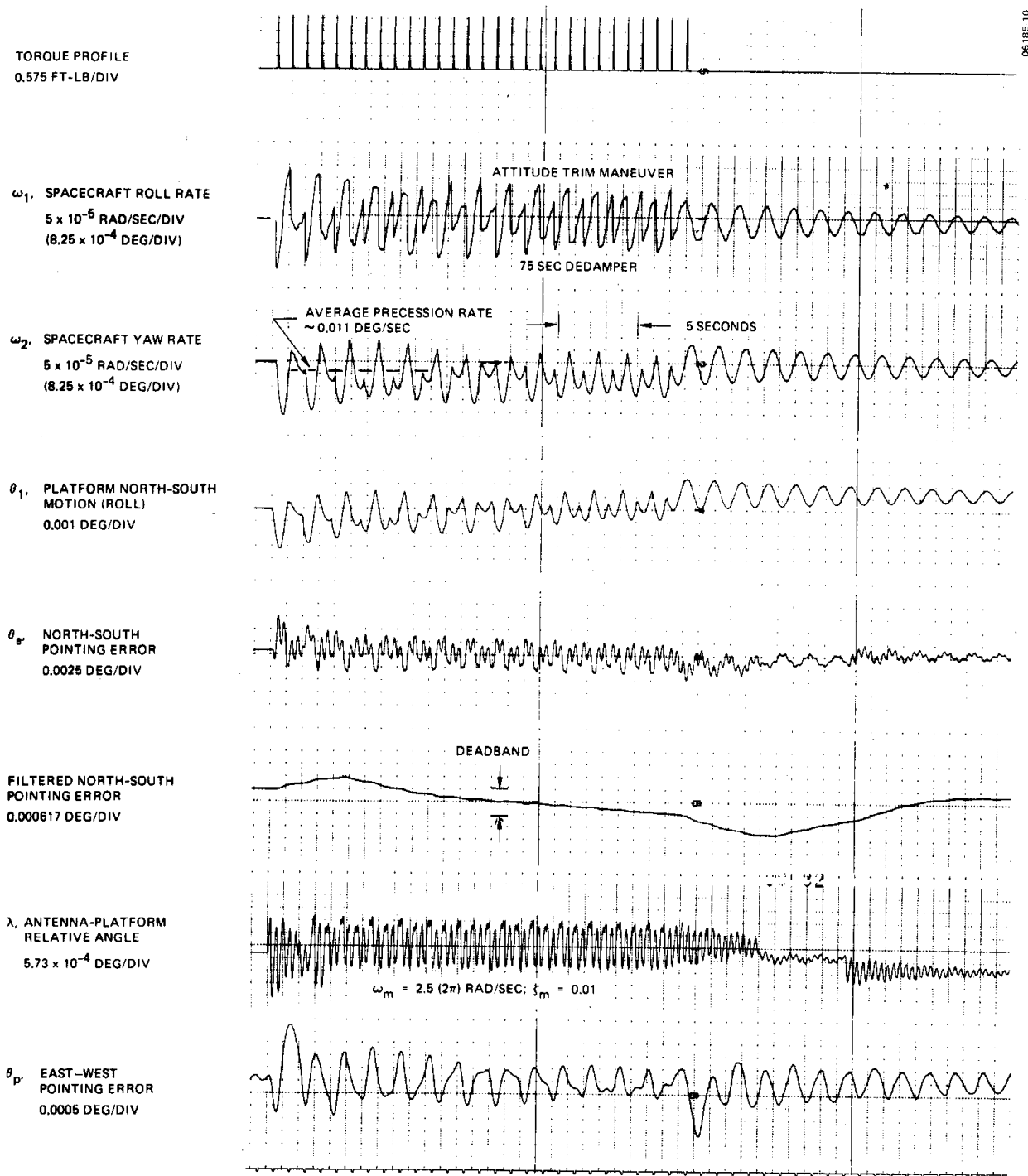


Figure 5. Vehicle Dynamics During Attitude Trim Maneuver

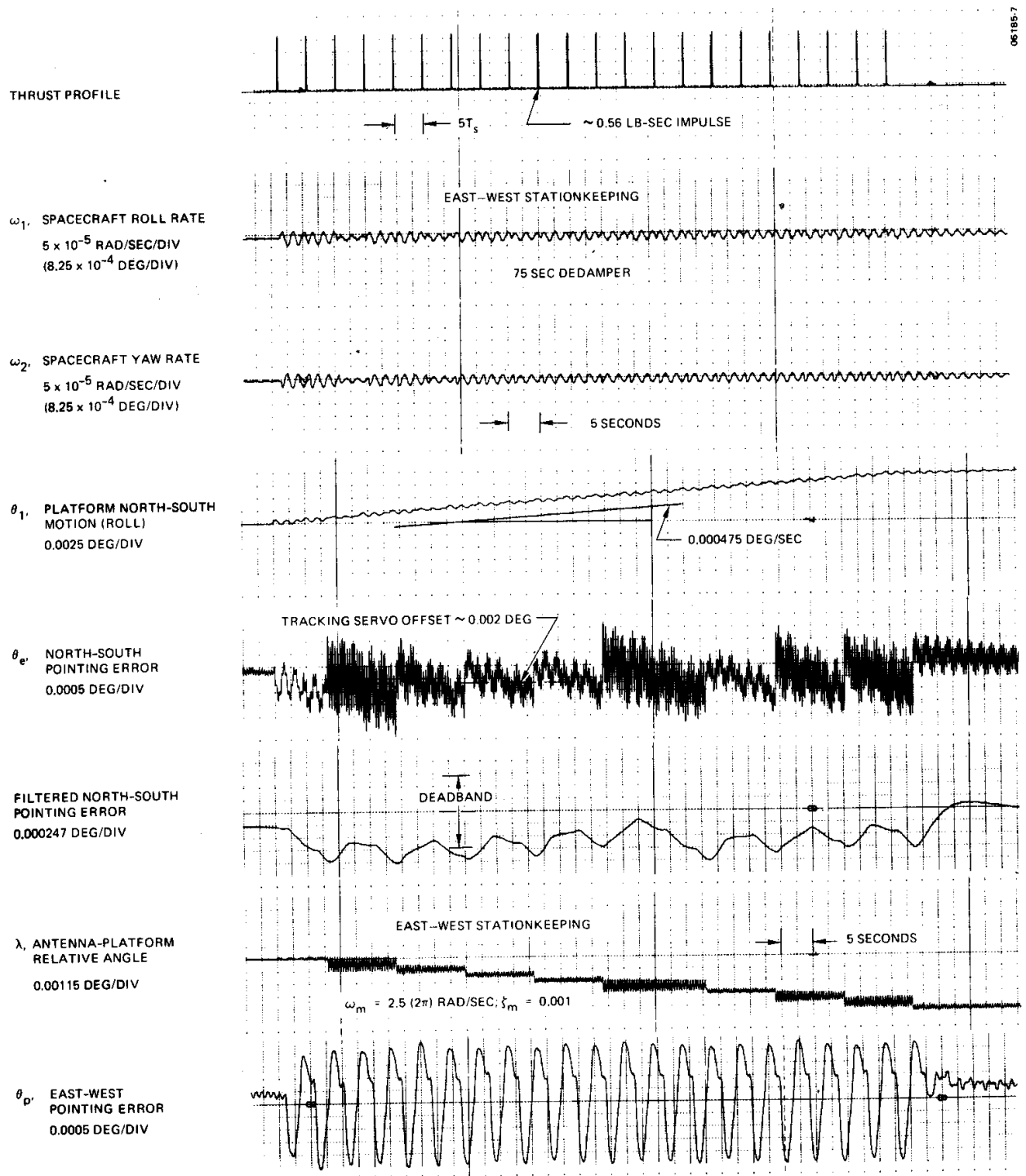


Figure 6. Vehicle Dynamics During East-West Velocity Maneuver

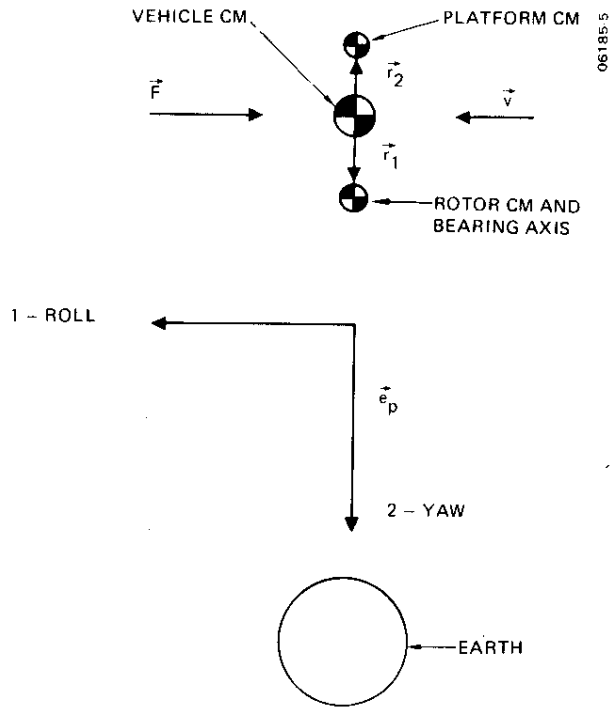


Figure 7. Mass Center and Spin Axis Positions in Steady State Pointing

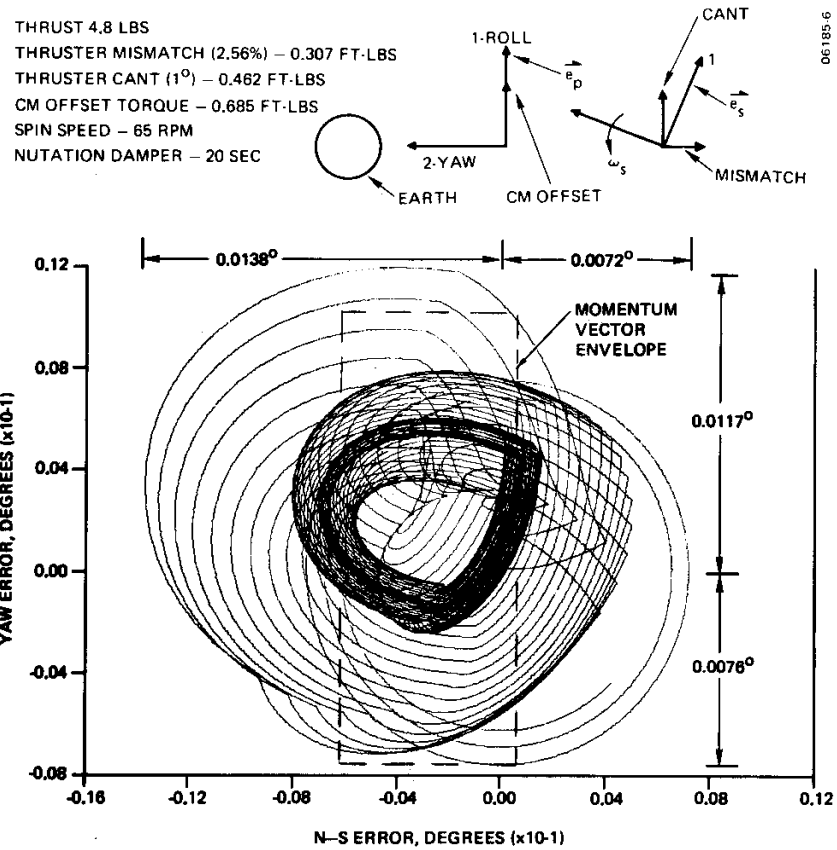


Figure 8. Motion of Spin Axis on an Inertial Plane During North-South Velocity Maneuver

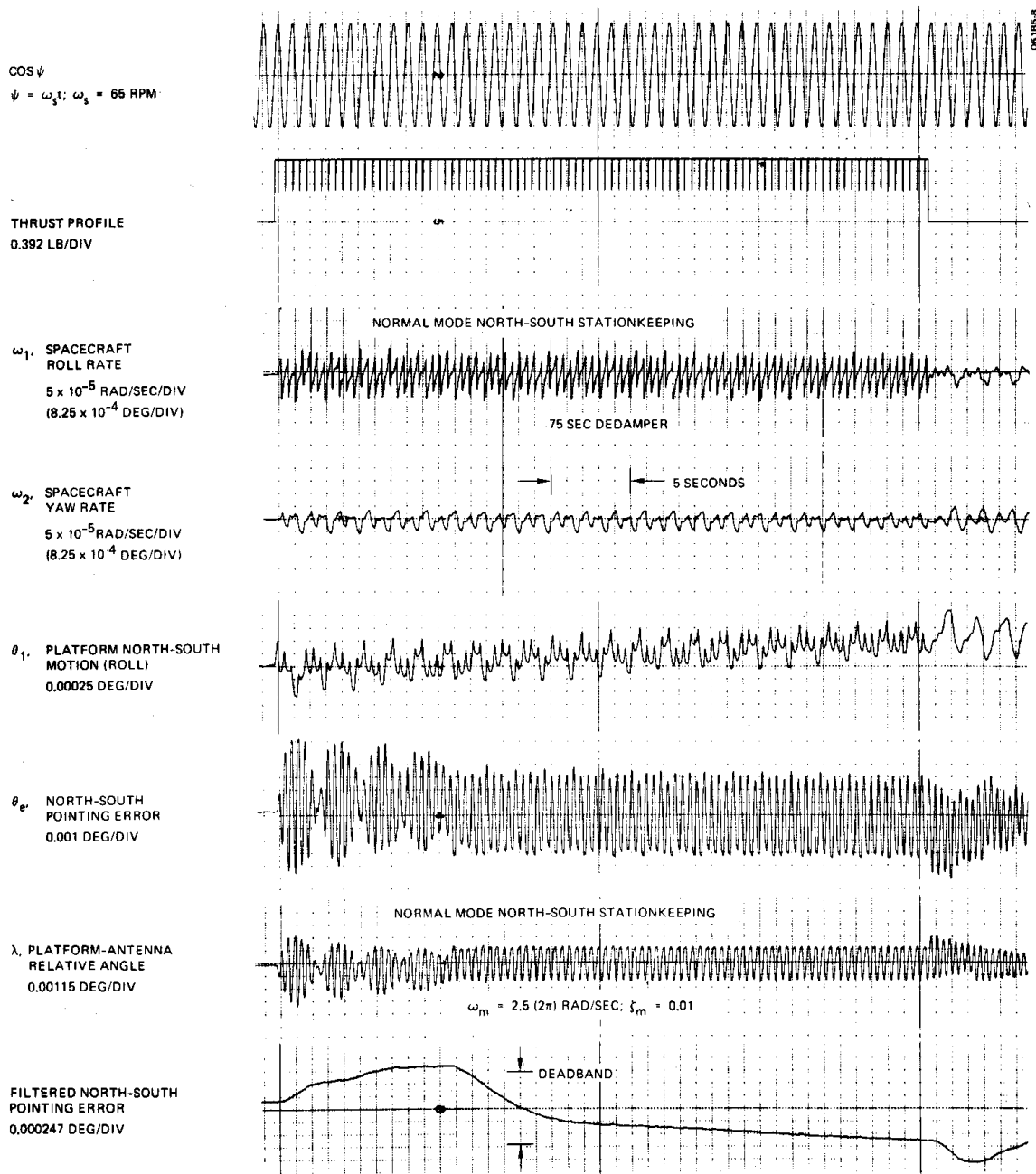


Figure 9a. Vehicle Dynamics During North-South Velocity Maneuver

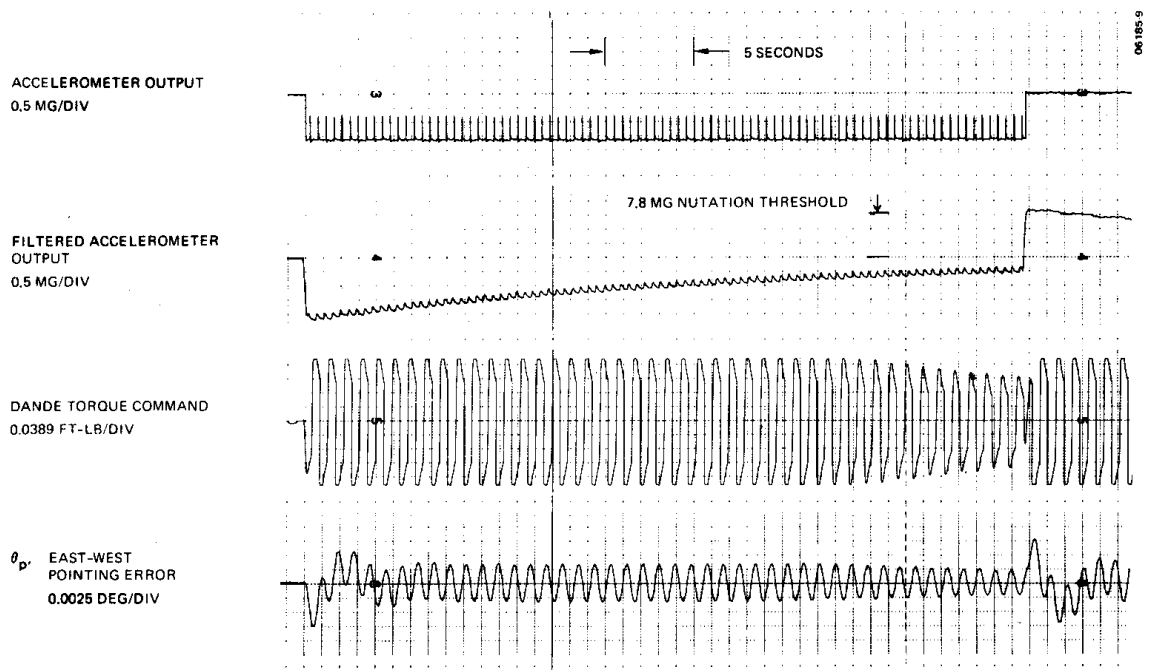


Figure 9b. Vehicle Dynamics During North-South Velocity Maneuver